PRAMANA
— journal of
physics

Vol. 54, No. 3
March 2000
pp. 431–440

Optical properties of 1T and 2H phases of TaS_2 and $TaSe_2$

SANGEETA SHARMA, S AULUCK and M A KHAN*
Department of Physics, University of Roorkee, Roorkee 247 667, India
*Institut de Physique et Chimie des materiaux Metalliques, 23, rue du loess, F-67037 Strasbourg Cedex, France

MS received 18 February 1999; revised 14 October 1999

Abstract. We have calculated the anisotropic frequency dependent dielectric function for the 1T and 2H phases of TaS_2 and $TaSe_2$ using the linear muffin tin orbital method within the atomic sphere approximation. We find significant anisotropy in the frequency dependent dielectric function for the 1T and 2H phases at low energies (less than 4 eV). Unfortunately there are no experimental data to compare with. The averaged dielectric function agrees with the available experimental data except that the calculated peak heights are underestimated and shifted to higher energies by 1–2 eV.

Keywords. Optical properties; LMTO-ASA; transition metal dichalcogenides.

PACS Nos 78.20-e; 78.20.Ci

1. Introduction

During the past three decades there has been a lot of interest in the structural, optical, electromagnetic and superconducting properties of the transition metal dichalcogenide (TMDCs) layered compounds. These compounds have a formula TX_2, where T is transition metal atom from group IVB, VB or VIB of the periodic table and X is one of the chalcogens (S, Se or Te). Wilson and Yoffe have reviewed the diverse physical properties of this broad class of materials [1]. Structurally, these compounds can be regarded as 2-dimensional (2D) X–T–X layers or sandwiches with intra-layer bonding strong and primarily covalent, while the inter-layer bonding is of the weak van der Waals type. The 2-dimensional nature of the bonding is responsible for a number of their unusual physical properties. For example, it is found that single crystals usually grow in the form of thin platelets, and these are readily cleaved to yield samples that are only a few hundred Å thick along the c-axis. Electrical and thermal conductivities are found to be significantly lower along the c-axis compared to in the basal plane.

The materials we are concerned with here are TaS_2 and $TaSe_2$. These have a hexagonal Bravais lattice with undistorted trigonal prismatic coordination in 2H polytypes and octahedral coordination in 1T polytypes. These compounds are of great interest because the behavior of resistivity, particularly of 1T TaS_2/Se_2 has been termed anomalous because the proposed band structure of 1T materials by Wilson and Yoffe predicts a partially

filled high density of states (DOS) d-band metal. The TMDCs formed from group IVB and VIB transition metal atoms exhibit semi-conducting or insulating properties, whereas these compounds (1T and 2H TaS_2/Se_2) tend to be metallic and become superconducting at low temperatures. The 2H phase is stable at room temperature while the 1T phase is stable at 800°C. Other polytypes have been identified (6R, 4H(a), 4H(b) and 4H(c)) [2]. Wilson *et al* [3] have focused in some detail, on the changes (structural, magnetic, optical, thermal etc) which occur in these materials at a variety of first order and second order transitions. They have associated this anomalous behavior with a nearly 2D Fermi surface (FS) supporting charge density wave (CDW) formation which introduces periodic lattice distortion [3]. Particularly for the 1T polytypes the Fermi surface (FS) is very simple and 2D in character with large nearly parallel walls. Such a situation theoretically favors the formation of CDW. Wilson *et al* found that when these waves first appear, the CDWs in the 1T polytypes are incommensurate with the lattice. This condition produces a fair amount of gapping in the DOS at E_{F} the Fermi level. For the simplest case of 1T-$TaSe_2$, the room temperature superlattice is realized when the existing CDW rotates into an orientation from which it then becomes commensurate. For 2H polytypes though, CDW formation is withheld to low temperatures, probably because of the more complex band structure. These observations further demonstrate the distinctiveness of these compounds.

These compounds have been a subject of photoemission studies [4,5]. The optical properties of group VA TMDC have been studied by transmission and reflectivity measurements in the visible and near infra-red parts of the spectrum at room temperature and liquid nitrogen temperature. Liang *et al* [6] have measured the room temperature reflectance of 1T Ta dichalcogenides and $TiSe_2$ alloyed with $TaSe_2$. Beal *et al* [7] have measured normal incidence reflectivity spectra in photon energy range 25 meV to 14 eV for the basal planes of single crystals of 2H-$NbSe_2$, 2H-$TaSe_2$, 2H-TaS_2 and 1T-TaS_2. The more recent studies on these layered compounds involve the study of bulk and surface electronic structure of 1T-TiS_2/Se_2 by Fang *et al* [8]. Spijkerman *et al* [9] have used x-ray scattering to identify a domain structure which is commensurate with a $\sqrt{13}a \times \sqrt{13}a$ structure in 1T-TaS_2. Kim *et al* [10] have observed a phase transition to the H phase induced by a STM tip in 1T-TaS_2. The STM image shows the characteristic triangular phase boundary between the original T phase ($\sqrt{13}a \times \sqrt{13}a$ CDW superstructure) and the 2H phase. Mandizabal *et al* [11] have reported a molecular modeling of lithium intercalated 1T-TiS_2.

Several semi-empirical band structure and ligand field models have been proposed to describe the electronic states in the layered compounds. Wilson and Yoffe [1] have discussed a schematic energy band model for several groups of TX_2 compounds. Later Bromley and Yoffe [12] have applied the semi-empirical tight binding (TB) method to calculate the band structure. Mattheiss [13] has used the augmented plane wave (APW) method to determine the electronic energy bands of 1T and 2H-TaS_2 and other similar compounds. Wexler and Woolley [14] have performed non-relativistic calculations for the band structure of 2H-TaS_2/$TaSe_2$ using the layer method within the muffin tin approximation. Myron and Freeman [15] have used the Korringa–Kohn–Rostoker (KKR) method in the muffin tin approximation to calculate the band structure and Fermi surface (FS) of 1T-TaS_2/Se_2. All these band calculations are non self-consistent and there is no detail calculation of the optical properties. There is one model optical calculation done by Beal *et al* [7]. They calculated the joint density of states (JDOS) by performing Kramers–Kröning analysis of electron energy-loss measurements on these materials by Bell and Liang [16].

Although there exist a large number of band structure calculations and experimental data on the optical properties of this important class of materials, there are no detailed calculations of the optical properties. In this paper we address ourselves to the calculation of the optical properties using the LMTO–ASA method. Optical properties calculated using LMTO–ASA method are found to be not significantly different from those calculated using the state of art full potential methods for metallic systems [17]. We have thus done calculations using LMTO–ASA method as it requires less computer time. We have calculated the optical properties of TaS_2 and $TaSe_2$ in the 1T and 2H phases. Our work will throw light on the effect of replacing Se by S and of changing stacking sequence in the frequency dependent dielectric function. A detailed comparison will be made with the experimental data of Beal *et al* [7].

In §2 we present the details of calculations. Section 3 includes the calculated optical dielectric function and comparison with experimental data. In §4 we summarize our calculations.

2. Details of calculation

These compounds have a hexagonal Bravais lattice. For the 2H phase we have undistorted trigonal prismatic coordination in 2H polytypes (space group $D^{\,4}_{6h}$ (P^6_3/mmc)). The unit cell in the c-direction spans two sandwiches. The Ta atoms are located at (0, 0, z) and S/Se atoms at (1/3, 2/3, u) and (1/3, 2/3, $1-u$) where $u = (1+z)/2$. For 1T polytypes (space group D^3_{3d} P_{3m1} Ta atom is octahedrally coordinated with S/Se atoms with only one sandwich in the unit cell. The Ta atom is located at (0, 0, 0) and S/Se atom at (1/3, 2/3, z). The lattice parameters, electronic configuration, and the WS radii are listed in table 1. We have used the ideal $z = 1/4$ in both structures because the experimental value of z are not very different from the ideal case.

The reliability of band structure methods based on the muffin tin approximation is best for closely packed structures. TaS_2/Se_2 compounds in the 1T structure have a packing fraction of about 34%. To make it amenable to band structure calculations Coehoorn *et al* [18] have done calculations with one empty sphere (Es) located at the position (0, 0, 1/2). This increases the packing fraction to about 45%. We have tried to include more Es to increase the packing fraction but found that in all cases the packing fraction decreases as compared to the one Es case. Hence we have performed calculations with one Es in 1T phase and two Es in the 2H phase because this gives the most closely packed structure.

Table 1. Lattice parameters in Å and Wigner Seitz radius in atomic units for 1T and 2H polytypes.

Polytype	Lattice constant (Å)	c/a	WS radius
1T-TaS_2	3.365	1.739	2.9507
1T-$TaSe_2$	3.477	1.804	3.2810
2H-TaS_2	3.316	3.640	3.1378
2H-$TaSe_2$	3.434	3.698	3.2672

It was suggested by Fang *et al* [8] that by choosing the Wiegner Sietz (WS) radius judiciously one can minimize 3PV and obtain a band structure close to that obtained by the state of art full potential methods. Fang *et al* found that this requires different Wiegner Sietz radii for Ti and S/Se in 1T TiS_2/Se_2 compounds. We have done calculations for 1T TaS_2 with one Es and using equal WS radii for Ta, S and Es atoms. The calculated band structure agrees very well with the full potential results with one band cutting $E_{\rm F}$ [17] in agreement with the previous calculations by Myron and Freeman. When the WS radii were made unequal the agreement with the full potential calculations worsens. Thus we have performed all the calculations using one Es for 1T polytypes and two Es for 2H polytypes and with equal WS radii for the constituent atoms and Es.

The scalar relativistic LMTO calculations are done within the atomic sphere approximation and including the combined correction terms. The Barth Hedin [19] exchange correlation potential is used. Calculations are done by expanding the wave functions at Ta and S/Se sites up to $l = 2$ (s, p, d). The WS radius is taken to be the same for both the atomic species. The one electron self-consistent potentials are obtained by performing iterations on a mesh of 196 k-points in the irreducible Brillouin zone (IBZ). We have used the tetrahedron method [20] for performing BZ summations. For a hexagonal structure we need to calculate two components of the frequency dependent dielectric function $\epsilon_{\parallel}(\omega)$ and $\epsilon_{\perp}(\omega)$ corresponding to the electric field parallel and perpendicular to the c-axis. Calculations of dielectric function involve the energy eigenvalues and electron wave functions. These are natural outputs of band structure calculations. We have thus performed calculations of the frequency dependent dielectric function of these compounds using expressions

$$\mathrm{Im}\,\epsilon_{\parallel}(\omega) = \frac{12}{m\omega^2}\int_{\rm BZ}\sum\frac{|P^Z_{nn'}(k)|^2\mathrm{d}S_k}{\nabla\omega_{nn'}(k)} \tag{1}$$

and

$$\mathrm{Im}\,\epsilon_{\perp}(\omega) = \frac{6}{m\omega^2}\int_{\rm BZ}\sum\frac{[|P^X_{nn'}(k)|^2 + |P^Y_{nn'}(k)|^2]\mathrm{d}S_k}{\nabla\omega_{nn'}(k)}, \tag{2}$$

where ω is the photon energy and $P^X_{nn}(k)$ is the x component of the dipolar matrix elements between initial $|nk>$ and final $|nk>$ states. $E_n(k)$ and $E_n(k)$ are the respective eigenvalues, $\omega_{nn}(k)$ is the energy difference and S_k is a constant energy surface. We have done calculations using 405 k-points in IBZ. The total dielectric function is given by

$$\mathrm{Im}\,\epsilon_{\rm tot}(\omega) = \frac{\mathrm{Im}\,\epsilon_{\parallel}(\omega) + 2\mathrm{Im}\,\epsilon_{\perp}(\omega)}{3}. \tag{3}$$

3. Optical properties

3.1 *1T polytypes*

We show the calculated $\epsilon_2(\omega)$ for the different polarizations of 1T-TaS_2 in figure 1a. The low energy peak at around 2 eV is due to $\epsilon_2^{\parallel}(\omega)$, while the higher energy structures beyond 4 eV have almost equal contributions from both polarizations thus resulting in an isotropic

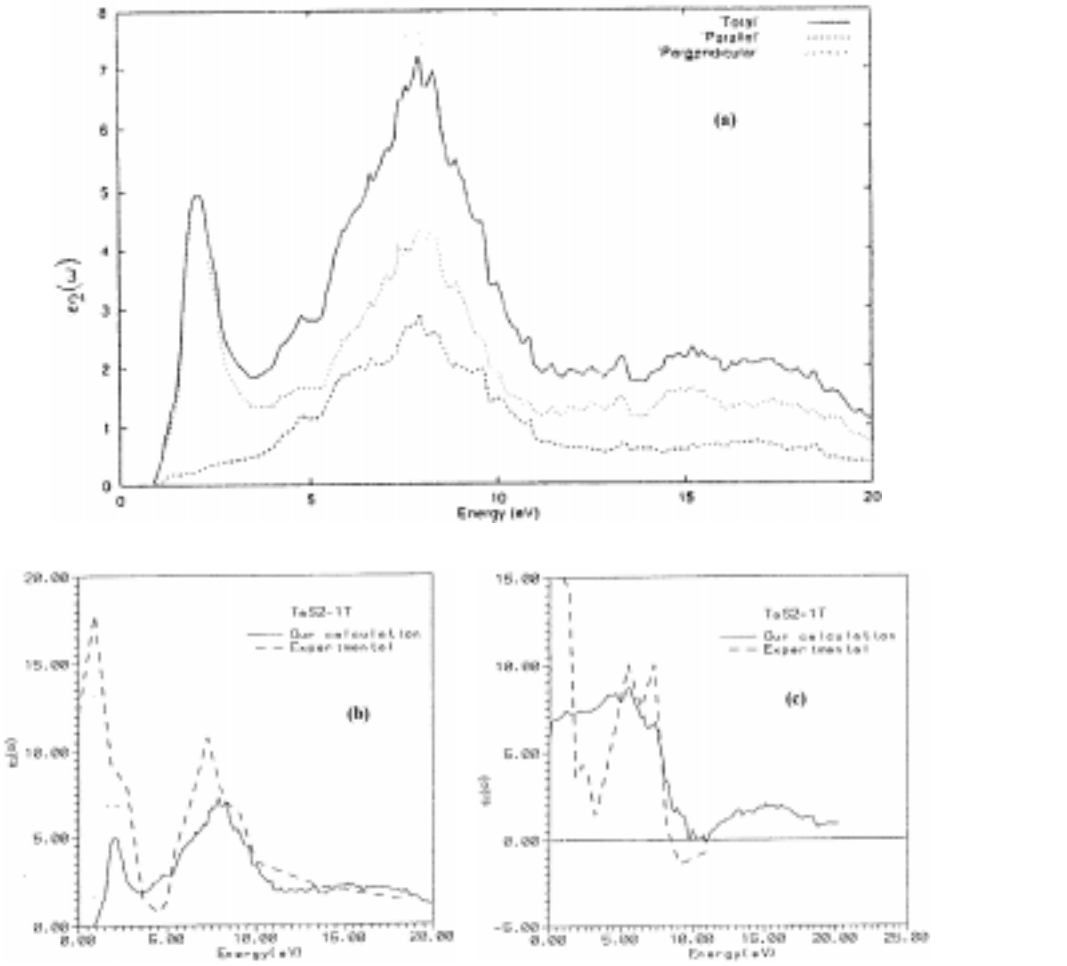

Figure 1. (**a**) Calculated average $\epsilon_2(\omega)$ (——), $\epsilon_2^{\parallel}(\omega)$ (- - -) and $\epsilon_2^{\perp}(\omega)$ (.....) for 1T-TaS_2; (**b**) calculated $\epsilon_2(\omega)$ for 1T-TaS_2. The experimental data of Beal *et al* (.....); (**c**) calculated $\epsilon_1(\omega)$ for 1T-TaS_2. The experimental data of Beal *et al* (.....).

behavior. It would be worthwhile to see how this is borne out by the experimental data. There are no measurements of $\epsilon_2^{\parallel}(\omega)$ and $\epsilon_2^{\perp}(\omega)$ for TaS_2/$TaSe_2$ compounds. We have therefore compared our averaged $\epsilon_2(\omega)$ with the experiment. The calculated $\epsilon_2(\omega)$ for 1T-TaS_2 is plotted in figure 1b along with experimental data of Beal *et al*. The calculated $\epsilon_2(\omega)$ has two pronounced peaks with the lower peak around 2 eV and higher around 8 eV and a minimum around 3 eV. The experimental data for 1T-TaS_2 shows two peaks around 1 eV and 7 eV, a minimum at 5 eV and a hump around 2.5 eV, which is missing in our calculations. Thus our calculated peaks are shifted to higher energies by around 1 eV. The peak around 2 eV is very small as compared to the experimental data. This could be due to the fact that we have not included the Drude term. In the higher energy regime (> 10 eV) both experiment and theory show featureless monotonically decreasing behavior.

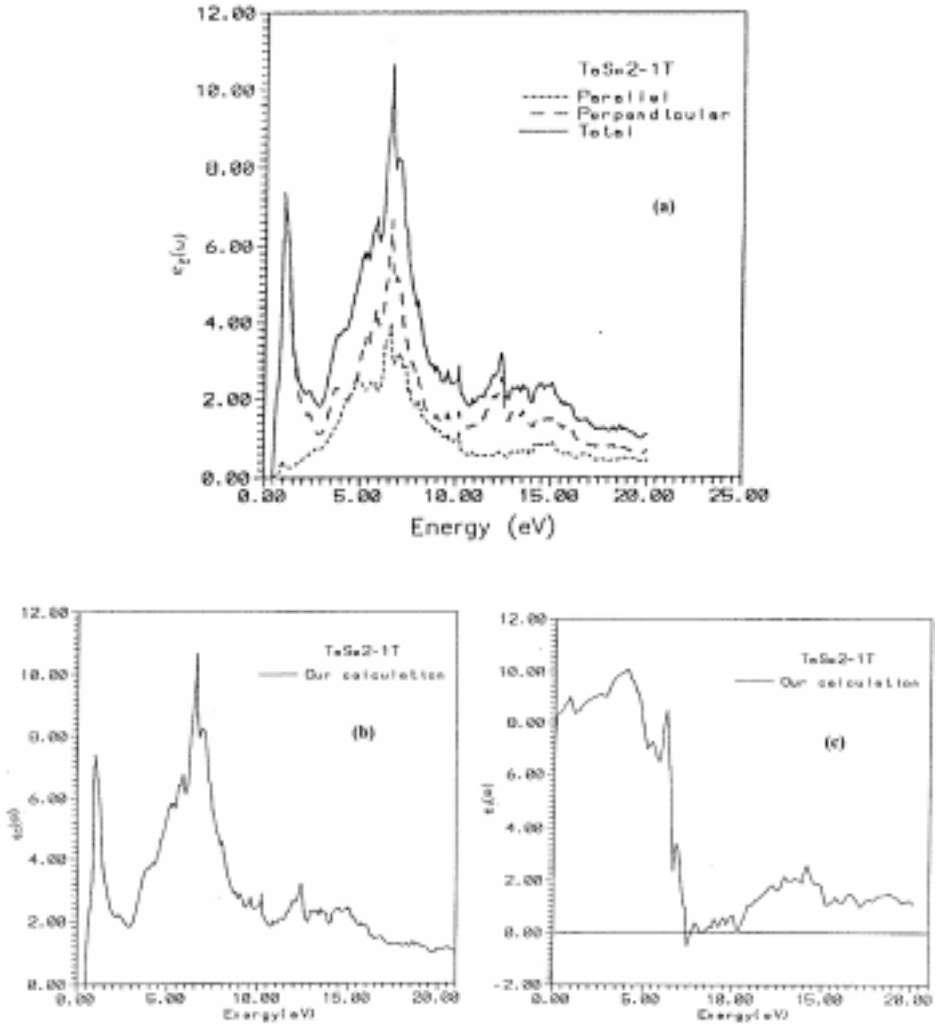

Figure 2. (**a**) Calculated average $\epsilon_2(\omega)$(——), $\epsilon_2^{||}(\omega)$ (.....) and $\epsilon_2^{\perp}(\omega)$ (- - -) for 1T-$TaSe_2$; (**b**) calculated $\epsilon_2(\omega)$ for 1T-$TaSe_2$; (**c**) calculated $\epsilon_1(\omega)$ for 1T-$TaSe_2$.

In order to identify the origin of the structures in $\epsilon_2(\omega)$ we have decided to take a simple approach, and that is that structure in $\epsilon_2(\omega)$ usually arises from a set of parallel bands over a sufficient region in k space. Our band structure is very similar to the previous calculated band structure of Mathiesis *et al* [13]. Thus looking at band structure [13] one could try to identify the origin of structures in $\epsilon_2(\omega)$. We see parallel bands along ΓA, KH, ML (because of 2D character), around Γ and along MK. These bands can give peaks around ∼2 eV (band 8, 9 to 10, 11, along ΓA and around Γ) and ∼8 eV (from band 4, 5 to 13 along ΓA and from 5 to 11 along MK).

From imaginary part of dielectric function $\epsilon_2(\omega)$ the real part is calculated using Kramers–Kröning relation [21].

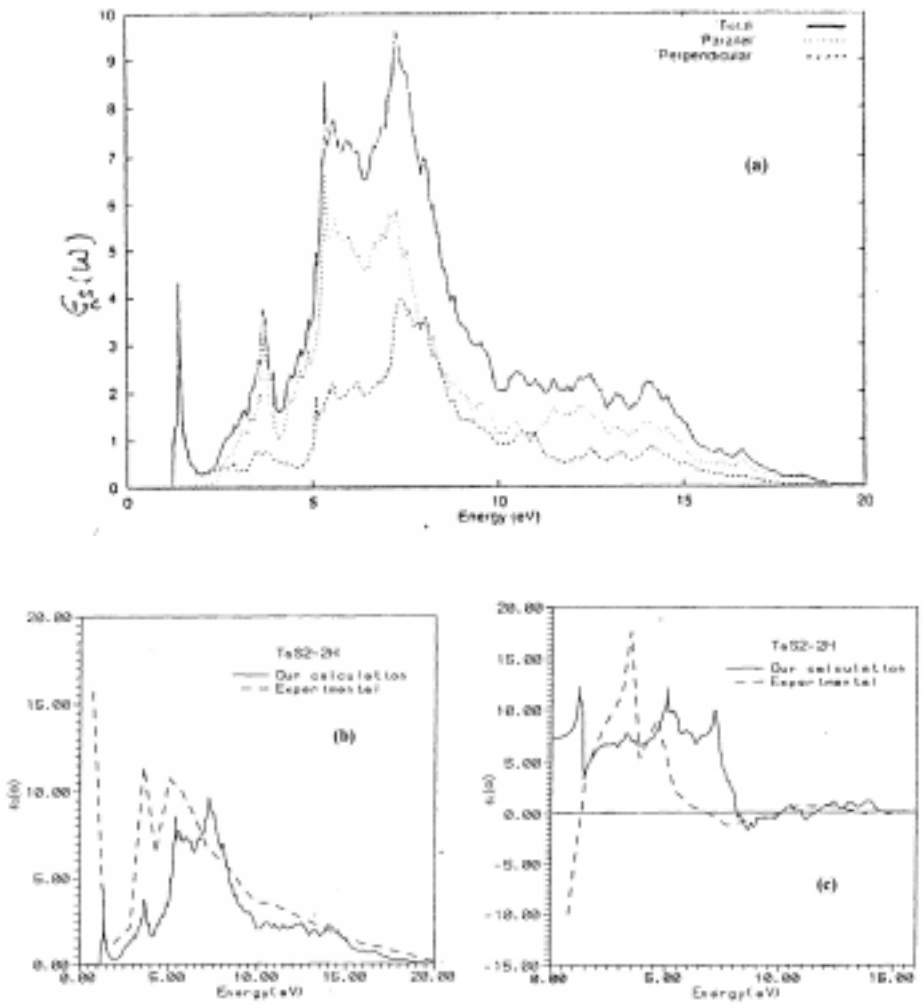

Figure 3. (**a**) Calculated average $\epsilon_2(\omega)$ (——), $\epsilon_2^{||}(\omega)$ (- - -) and $\epsilon_2^{\perp}(\omega)$ (.....) for 2H-TaS_2; (**b**) calculated $\epsilon_2(\omega)$ for 2H-TaS_2. The experimental data of Beal *et al* (.....); (**c**) calculated $\epsilon_1(\omega)$ for 2H-TaS_2. The experimental data of Beal *et al* (.....).

$$\epsilon_1(\omega) = 1 + \frac{2}{\pi} P \int_0^{\infty} \frac{\omega' \epsilon_2(\omega')}{(\omega')^2 - \omega^2} \mathrm{d}\omega'. \tag{4}$$

Here P indicates principal value of the integral. The calculated $\epsilon_1(\omega)$ for 1T-TaS_2 is presented in figure 1c. Dashed line is the experimental data of Beal *et al*. The calculated $\epsilon_1(\omega)$ has a broad peak around 5 eV, in experimental data there is a twin peak around 7 eV. Our calculated peaks are shifted to lower energies by around 1.5 eV. The calculated $\epsilon_1(\omega)$ crosses zero at 9.7 eV while experimental data crosses zero at 8.5 eV. This shows a shift in higher energy side by around 1–2 eV. The calculated $\epsilon_1(\omega)$ fails to give the low energy

peak. This could be because of non-inclusion of the Drude term which gives a major contribution in low energy regime and also because we are unable to estimate the correct magnitude of low energy peak in $\epsilon_2(\omega)$.

The anisotropic dielectric functions for 1T-$TaSe_2$ are plotted in figure 2a and the $\epsilon_2(\omega)$ in figure 2b. The $\epsilon_1(\omega)$ in figure 2c has two main features one larger at 3.5 eV and smaller at ∼6 eV and $\epsilon_1(\omega)$ crosses zero at ∼7.5 eV. This is interpreted as excitation of plasmons. We are not aware of any experimental data to compare our results with.

3.2 *2H-polytypes*

The calculated anisotropic/averaged $\epsilon_2(\omega)$ for 2H-TaS_2 and $TaSe_2$ are presented in figures 3a, b and 4a, b respectively. As compared to the results of 1T-polytypes these show a

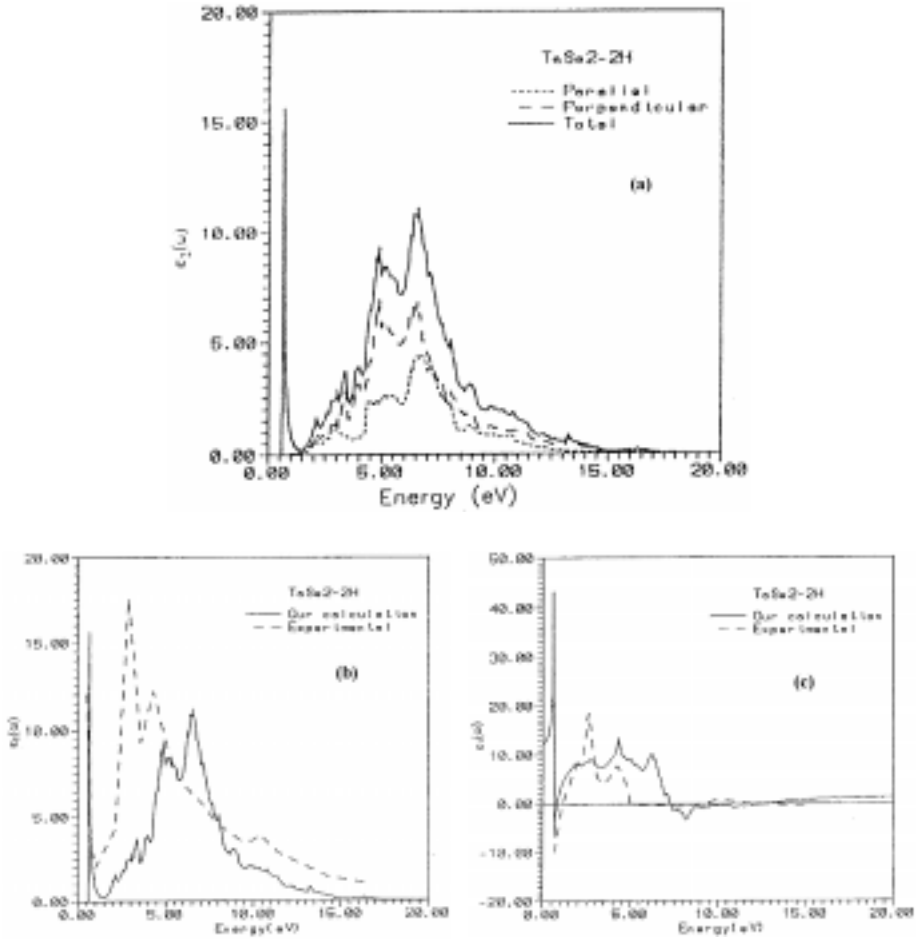

Figure 4. (**a**) Calculated average $\epsilon_2(\omega)$ (——), $\epsilon_2^{||}(\omega)$ (.....) and $\epsilon_2^{\perp}(\omega)$ (- - -) for 2H-$TaSe_2$; (**b**) calculated $\epsilon_2(\omega)$ for 2H-$TaSe_2$. The experimental data of Beal *et al* (.....); (**c**) calculated $\epsilon_1(\omega)$ for 2H-$TaSe_2$. The experimental data of Beal *et al* (.....).

splitting of the main peak (6 eV for 1T-TaS_2) into two peaks with the lower peak around 5 eV and higher around 7 eV. In both the cases these peaks are lower in magnitude and shifted to higher energy by around 2 eV as compared to the experimental data [7]. $\epsilon_2(\omega)$ further shows a peak around ∼1.5 eV, in case of 2H-TaS_2 this peak is small but it is very large in magnitude in 2H-$TaSe_2$. Both the curves show a featureless behavior in the higher energy regime (>10 eV). The calculated $\epsilon_2(\omega)$ for 2H-TaS_2 shows a low energy peak at ∼2 eV is due to $\epsilon_2^{\parallel}(\omega)$ while the peak at ∼4 eV is mainly due to $\epsilon_2^{\perp}(\omega)$. Beyond 5 eV both polarizations show similar isotropic behavior.

The origin of these peaks can be identified by a set of parallel bands along ΓA, MK, ML and around Γ. These bands could give structures ∼2 eV (16 to 18 along ΓM), ∼5 eV (16 to 24 along ΓM), ∼7 eV (12, 13 to 18 along MK and 13 to 18 along ΓM).

The calculated $\epsilon_1(\omega)$ along with experimental data is presented in figure 3c, for 2H-TaS_2 and figure 4c for 2H-$TaSe_2$. In both the cases the calculated peaks (∼5 eV and ∼7 eV) are shifted to higher energies by around 2 eV with respect to the experimental data and the first peak (∼5 eV) is lower in magnitude as compared to data of Beal *et al* while the second peak (∼7 eV) is higher in magnitude. In the low energy regime (∼1 eV) non-inclusion of the Drude term causes discrepancy between the experimental data and our calculation. The calculated peak position and heights are almost similar for both TaS_2 and $TaSe_2$.

4. Conclusions

In this article we have presented the results of the optical properties for 1T and 2H phases of TaS_2 and $TaSe_2$ using the LMTO–ASA method [22]. We have explored the effect of Es which is by now the standard way to increase the packing fraction and thus increase the acceptability of the LMTO–ASA calculations. In this respect we find that our calculations with one Es for 1T polytypes and two Es for 2H polytypes results in maximum packing fraction and the results match closely with state of art full potential calculations [17].

The calculated $\epsilon_2(\omega)$ for 1T-TaS_2 is in agreement with the experimental data except that our calculated peaks are shifted to higher energies by 1–2 eV and the peak heights are underestimated as compared to the experimental data. The inclusion of the intraband transitions could lead to improved agreement. The $\epsilon_1(\omega)$ is in better agreement with the experimental data except at low energies. The $\epsilon_2(\omega)$ for the 1T-$TaSe_2$ is very similar to the $\epsilon_2(\omega)$ for 1T-TaS_2. The $\epsilon_2(\omega)$ for the 2H-TaS_2 is in good overall agreement with the experimental data, the calculated peak positions are shifted to higher energies by ∼2 eV as compared to the experimental data. This could well be related to the underestimate of the energy gap in the local density approximation (LDA). The peak heights for 2H-TaS_2 are in better agreement with the experimental data as compared to 2H-$TaSe_2$. In going from 1T to 2H phase the single main peak is split into two peaks. This is indicative of doubling of bands. The peaks have been identified as arising from parallel set of bands. In 1T-polytypes the peaks are ∼2 eV (8, 9 to 10, 11, along ΓA and around Γ), ∼8 eV (4, 5 to 13 along ΓA and 5 to 11 along MK). In case of 2H-polytypes the peaks are ∼2 eV (16 to 18 along ΓM), ∼5 eV (16 to 24 along ΓM), ∼7 eV (12, 13 to 18 along MK and 13 to 18 along ΓM).

Acknowledgement

These calculations are done at New Computing Facilities and at the Physics Department Computing facilities. We are grateful to them. We are thankful to Council of Scientific and Industrial Research (CSIR), for financial support in the form of a grant no. 827.

References

[1] J A Wilson and A D Yoffe, *Adv. Phys.* **18**, 193 (1969)
[2] J V Landuyt, G V Tendeloo and S Amelinckx, 1974 *Phys. Status Solidi* **A26**, 197 (1974); **36**, 767 (1976)
[3] J A Wilson, F J Di Salvo and S Mahajan, *Adv. Phys.* **24** 117 (1975)
[4] N V Smith and M M Traum, *Phys. Rev.* **B11**, 2087 (1975)
[5] M M Traum, N V Smith and F J Di Salvo, *Phys. Rev. Lett.* **32**, 1241 (1974)
[6] W Y Liang, G Lucovsky, R M White, W Stutius and K R Pisharody, *Philos. Mag.* **33**, 493 (1976)
[7] A R Beal, H P Hughes and W Y Liang, *J. Phys.* **C8**, 4236 (1975)
[8] C M Fang, R A de Groot and C Haas *Phys. Rev.* **B56**, 4455 (1997)
[9] Albert Spijkerman, J L de Boer, Auke Meetsma, G A Wiegers and S V Smaalen, *Phys. Rev.* **B56**, 13,757 (1997)
[10] Kim Ju-Jin , Park Chan, W Yamaguchi, O Shiino, K Kitazawa and T Hasegawa, *Phys. Rev.* **B56**, R15 573 (1997)
[11] Fernando Mendizabal, Renato Contreras and A Aziman, *J. Phys. Condens Matter* **9**, 3011 (1997)
[12] R A Bromley, R B Murray and A D Yoffe, *J. Phys.* **C5**, 759 (1972)
[13] L F Mattheiss, *Phys. Rev.* **B8**, 3719 (1973)
[14] G Wexler and A M Woolley, *J. Phys.* **C9**, 1185 (1976)
[15] H M Myron and A J Freeman, *Phys. Rev.* **B11**, 2735 (1975)
[16] M G Bell and W Y Liang, *Adv. Phys.* **25**, 52 (1976)
[17] Rajeev Ahuja *et al*, (private communication).
[18] R Coehoorn, C Haas, J Dijkstra, C J Flipse, R A de Groot and A Wold, *Phys. Rev.* **B35**, 6195 (1987)
[19] U Von Barth and L Hedin, *J. Phys.* **C5**, 1629 (1972)
[20] O K Andersen, *Phys. Rev.* **B12**, 3060 (1975)
[21] O Jepsen and O K Andersen, *Solid State Commun.* **9**, 1763 (1971)
G Lehmann and M Taut, *Phys. Status Solidi* **B54**, 469 (1972)
[22] O K Anderson, *Phys. Rev.* **B12**, 3060 (1975)